1

JUPITER'S MAGNETIC FIELD AND MAGNETOSPHERE

Mario H. Acuña, Kenneth W. Behannon, and J. E. P. Connerney

Jupiter has a magnetic moment second only to that of the Sun's. Estimates of dipole magnitude range from 4.208–4.28 G-R_J^3. The dipole is found to be tilted $\sim 9.6°$ to the rotation axis toward $\sim 202°$ System III (1965) longitude in the northern hemisphere. Jupiter also possesses substantial quadrupole and octupole moments, which implies that the interior sources of the field lie nearer the surface than in the case of Earth. The internally-produced field dominates the inner magnetosphere out to a distance of $\sim 6\ R_J$, the orbital distance of Io, where measurement of perturbation magnetic fields yields an estimated 2.8×10^6 A for the current flowing in the Alfvén current tube linking Io with the Jovian ionosphere. The middle magnetosphere of Jupiter, extending from $\sim 6\ R_J$ to 30–50 R_J, is dominated by an equatorial azimuthal current disc. When the disc is modeled as a 5 R_J thick annular current sheet extending from 5 to 50 R_J, a fit to spacecraft data requires a current density of $\sim 5 \times 10^6$ A/R_J^2 at the inner edge of the annulus. An asymmetric longitudinal variation in the radial component of the magnetic field in this region provides evidence for a thickening of the magnetodisc on the dayside. Between the outer edge of the disc and the sunward magnetopause, which can vary in distance from $\sim 45\ R_J$ to $\sim 100\ R_J$ there is a "buffer" zone which is very sensitive to variations to external pressure. The field there is southward on average, but highly variable in both magnitude and direction on timescales less than one hour, especially near the magnetopause. On the nightside of the planet, a magnetic tail of radius ~ 150–$200\ R_J$ and length of probably a few AU is formed in the interaction of the solar wind with the Jovian magnetosphere. The $\sim 5\ R_J$ thick current sheet separating the tail lobes is a night side extension of the magnetodisc, is on average parallel to the ecliptic plane and oscillates about the longitudinal axis of the tail as Jupiter rotates. In the dawn and tailward magnetosheath, the magnetic field has a predominant north–south orientation and varies between the two extremes with a quasiperiod of ~ 10 hr. There is strong correlation with the north–south plasma velocity components in those regions, suggesting convected wave production by the wobble of the flattened Jovian magnetosphere and current sheet system.

1.1. Introduction

Among the planets in the solar system, Jupiter is unique not only because of its immense size and mass and the variety of phenomena taking place in its environment, but also because of its large magnetic moment, second only to the Sun's. The Jovian magnetic field was first detected indirectly by radio astronomers who postulated its existence to explain observations of nonthermal radio emissions from Jupiter at decimetric and decametric wavelengths [see Chapter reviews and Carr and Gulkis, 1969; Carr and Desch, 1976; Berge and Gulkis, 1976; also de Pater, 1980b]. Some of the basic characteristics of the field were derived from these observations, such as its southward polarity, opposite Earth's, and the approximate value of the tilt angle between the magnetic dipole axis and the axis of rotation of the planet, determined to be $\sim 10°$. Coarse estimates were established for the surface field intensity and dipole moment based on trapped radiation models and the observed cutoff of decametric emissions at 40 MHz [Komesaroff, Morris, and Roberts, 1970; Carr, 1972a].

Since these early radio astronomical studies of the Jovian magnetosphere, four spacecraft, Pioneer 10 (1973), Pioneer 11 (1974), Voyager 1, and Voyager 2 (both

1979), have flown by the planet at close distances and have provided in situ information about the field geometry and its strength. The direct measurements confirmed the zeroth order models derived from the radio data and added a vast amount of new and detailed information about the global characteristics of the field, its dynamics and interaction with the solar wind. For detailed reviews of early results derived from ground based and the Pioneer 10 and 11 spacecraft observations the reader is directed to the book *Jupiter*, edited by Gehrels [1976], and to Smith and Gulkis [1979], Davis and Smith [1976], Acuña and Ness [1976a,b,c], and Carr and Gulkis [1969] and references therein.

As in the case of Earth, the magnetic field stands off the solar wind at a considerable distance from the planet, creating a giant magnetospheric cavity. If it were visible, the Jovian magnetosphere would appear from Earth to be the largest object in the sky. Viewed head on, its width would be about four times as large as the Moon or Sun. The boundary of this cavity comprises a detached bow shock wave, generated by the super-Alfvénic flow of the solar wind past the magnetized obstacle, a magnetosheath layer in which the deflected solar wind creates a turbulent flow regime, and a magnetopause "surface" at which internal magnetospheric pressure balances that associated with the impinging solar wind.

It has become customary to describe the Jovian magnetosphere in terms of three principal regions. The *inner magnetosphere* is the region where the magnetic field created by sources internal to the planet dominates, and contributions from current systems external to the planet are not significant. This region was initially defined as extending from the planetary surface to a distance of 10–15 R_J (Jovian radii), but recent results from the Voyager flybys indicate that the outer radius should be reduced to approximately 6 R_J, the orbit of Io. Outside of this region the effects of an azimuthal current sheet in the equatorial plane produce a significant perturbation, leading to the stretching of the magnetic field lines in the radial direction. The region in which the equatorial currents flow will be denoted as the *middle magnetosphere*, and in our definition, would extend from $\sim 6\ R_J$ to approximately 30–50 R_J where the asymmetry due to the magnetopause and tail current systems becomes important. In the *outer magnetosphere*, the field has a large southward component and exhibits large temporal and/or spatial variations in magnitude and direction in response to changes in solar wind pressure. This region extends from the magnetopause boundary to approximately 30–50 R_J, and includes as well the extensive Jovian magnetic tail.

In this chapter we shall present a description of the magnetic field in these three regions from the phenomenological point of view derived from spacecraft observations (predominantly the recent Voyager results) and the quantitative models which have been developed to date on the basis of these observations.

1.2. The inner magnetosphere

General description and mathematical models

As previously defined, the inner magnetosphere is that region where the magnetic field generated by currents flowing in the interior of the planet dominates. The time-scale for field variations, both in magnitude and direction, is long, and the field is smoothly varying when observed from a spacecraft in a flyby trajectory. It is generally accepted that the magnetic-field-generation mechanism is a thermal-convection-driven dynamo operating in the electrically conducting regions of Jupiter's interior [Hide and Stannard, 1976; Gubbins, 1974; Busse, 1979]. Thus knowledge about the magnetic field provides means for studying Jupiter's interior [Smoluchowsky, 1975; Stevenson,

1974]. Beyond 6 R_J the effects of external currents become too significant to be neglected; hence, we have chosen this radius as the outer boundary.

Because the region of interest contains no significant sources (i.e., $\mathbf{J} = \nabla \times \mathbf{B} \simeq 0$), the magnetic field $\mathbf{B}$ can, to good approximation, be derived from a scalar potential function V which represents the contribution of sources internal and external to the region. Thus, we have

$$\mathbf{B} = -\nabla V = -\nabla(V^e + V^i) \tag{1.1}$$

The potential function V is the sum of an external potential V^e and an internal potential V^i and is generally expressed in terms of spherical harmonic functions, that is, solutions to Laplace's equation of the form [Chapman and Bartels, 1940]

$$V = V^e + V^i = a \sum_{n=1}^{\infty} \left(\frac{r}{a}\right)^n T_n^e + \left(\frac{a}{r}\right)^{n+1} T_n^i \tag{1.2}$$

This is the classical formulation for the potential originated by Gauss in 1830 and used in studies of the Earth's magnetic field [Gauss, 1877]. In our case, r denotes the distance from Jupiter's center and a is Jupiter's equatorial radius, (1 R_J = 71,372 km). (A general discussion of the representation of magnetic fields in space has been given by Stern [1976].)

The functions T_n^e and T_n^i are given with respect to the coordinate system defined below, as:

$$T_n^e = \sum_{m=0}^{n} P_n^m(\cos\theta)\,[G_n^m \cos m\phi + H_n^m \sin m\phi] \tag{1.3}$$

for the contribution due to exterior sources and

$$T_n^i = \sum_{m=0}^{n} P_n^m(\cos\theta)\,[g_n^m \cos m\phi + h_n^m \sin m\phi] \tag{1.4}$$

for the internal sources.

The angles ϕ and θ are the conventional right-handed polar coordinates and therefore denote Jovigraphic System III (1965.0) *east* longitude and colatitude respectively, $P_n^m(\theta)$ are associated Legendre functions with Schmidt normalization and g_n^m, h_n^m, G_n^m, H_n^m are the Schmidt coefficients. In some studies the external potential V^e has been expressed in an inertial (nonrotating) coordinate system [see Smith et al., 1975].

If we assume a magnetic field representation of the form (1.1), the development of a magnetic field model from a set of M observations along a spacecraft trajectory requires the determination of the coefficients g_n^m, h_n^m, G_n^m, and H_n^m up to order $n = n_{\max}$ ($n_{\max} < \infty$) that minimize the sum of the vector residuals squared

$$X^2 = \sum_{k=1}^{M} |\mathbf{B}_{\text{model}}^{\,k} - \mathbf{B}_{\text{obs}}^{\,k}|^2 = \sum_{k=1}^{M} |\epsilon_k|^2 \tag{1.5}$$

The order of the model, $n = n_{\max}$, represents the physical complexity associated with the mathematical formulation. From potential theory it is known that a unique

Table 1.1. *Spherical harmonic coefficients for models of the Jovian magnetic field (System III, 1965)*

Terms		O_4 (Acuña and Ness, 1976)	P 11(3,2)*A*, Davis et al. (1975)
Internal:	g_1^0	4.218	4.144
	g_1^1	−0.664	−0.692
	h_1^1	0.264	0.235
	g_2^0	−0.203	0.036
	g_2^1	−0.735	−0.581
	h_2^1	−0.469	−0.427
	g_2^2	0.513	0.442
	h_2^2	0.088	0.134
	g_3^0	−0.233	−0.047
	g_3^1	−0.076	−0.502
	h_3^1	−0.580	−0.342
	g_3^2	0.168	0.352
	h_3^2	0.487	0.296
	g_3^3	−0.231	−0.136
	h_3^3	−0.294	−0.041
External:	G_1^0		−194.6 (nT)
	G_1^1		68.7
	H_1^1		80.3
	G_2^0		5.6
	G_2^1		9.1
	H_2^1		− 9.4
	G_2^2		− 16.2
	H_2^2		− 8.3

representation of the magnetic field in a source-free region is derivable from vector measurements over a simple surface that completely encloses the internal sources. Because a spacecraft trajectory only constitutes a single curve in space, the solutions obtained are not unique, and cross coupling or mutual dependence among the Schmidt coefficients occurs.

From the above, it is clear that trajectories that maximize the range of latitudes and longitudes covered within the radial distances considered lead to more complete representations of the planetary field. The characteristics of a given trajectory can be used to determine the order of the model n_{max} that can be used to model the observations with acceptable physical credibility. A model of the planetary field incorporating

Table 1.2. *Characteristics of dipole terms for models of the Jovian magnetic field*[a]

Model	$\|M\|$	Tilt	λ_{III} (1965)
O_4	4.28	9.6°	201.7°
P 11(3,2)*A*	4.208	10°	198.8°

[a] For the characteristics of dipole terms derived from other models of the field the reader is referred to *Smith and Gulkis* [1979].

terms of order higher than n_{max} may fit the data exceedingly well along the spacecraft trajectory, but not elsewhere. Hence, the predictive properties and basic purpose of the model are rendered useless. Detailed discussions on the selection of n_{max} for given spacecraft trajectories and the physical validity of higher order models have been given by Acuña and Ness [1976b], Davis and Smith [1976], and Connerney [1981a]. The latter author in particular has applied generalized inverse techniques to the least-squares problem represented by Equation (1.5), which yield direct estimates of confidence levels associated with the Schmidt coefficients for a given spacecraft trajectory.

In the case of Jupiter, the best trajectory for planetary magnetic field studies was that provided by Pioneer 11. This was a high latitude retrograde flyby with a closest Jovicentric approach distance of 1.6 R_J. Although Pioneer 10 and Voyager 1 approached the planet to within 2.85 and 4.9 R_J respectively, their prograde trajectories remained close to the equatorial plane; Voyager 2 only came to within 10 R_J of Jupiter and thus did not contribute significant data for studies of the planetary field. However, these latter three spacecraft provided a wealth of information about the middle magnetosphere and hence, indirectly, about the radial distance range over which the spherical harmonic representation is valid [Davis and Smith, 1976; Ness et al., 1979a,b,c].

On the basis of the Pioneer 10 and 11 measurements [Smith et al., 1975; Acuña and Ness, 1976a,b,c], several models of the Jovian magnetic field were developed. Each of these reflects not only the many approaches that are possible in obtaining estimates for the spherical harmonic coefficients, but they also point to slight measurement differences in the respective observations [Acuña and Ness, 1976c; Davis and Smith, 1976; Connerney, 1981a]. Two principal models have emerged as "best" representing the planetary field in terms of spherical harmonics: the O_4 model of Acuña and Ness [1976a,c] and the P 11(3,2)*A* model of Davis, Jones, and Smith [1975] (see also Smith, Davis, and Jones [1976]). They have been tested against independent evidence from ground based radio observations and in situ energetic-charged-particle measurements. The latter provide information about the global characteristics of the field not obtainable from the local magnetic field measurements and hence lend physical credibility to the models [Acuña and Ness, 1976a,c; Smith and Gulkis, 1979]. Table 1.1 lists the Schmidt coefficients for both models. The O_4 model includes terms up to the octupole ($n_{max} = 3$) but no external terms ($G_n^m = H_n^m \equiv 0$). The P 11(3,2)*A* model also includes internal terms up to the octupole but adds external terms which include quadrupole coefficients ($n_{max}^{ext} = 2$). These coefficients have been transformed to the System III (1965) longitude system values. The characteristics of the dipole terms are given in Table 1.2.

The global characteristics of the field predicted by these models are illustrated in Figures 1.1 through 1.3 where the total field intensity, dip, and declination angles are shown in the form of isocontour maps at the surface of the planet and at 2 Jovian radii.

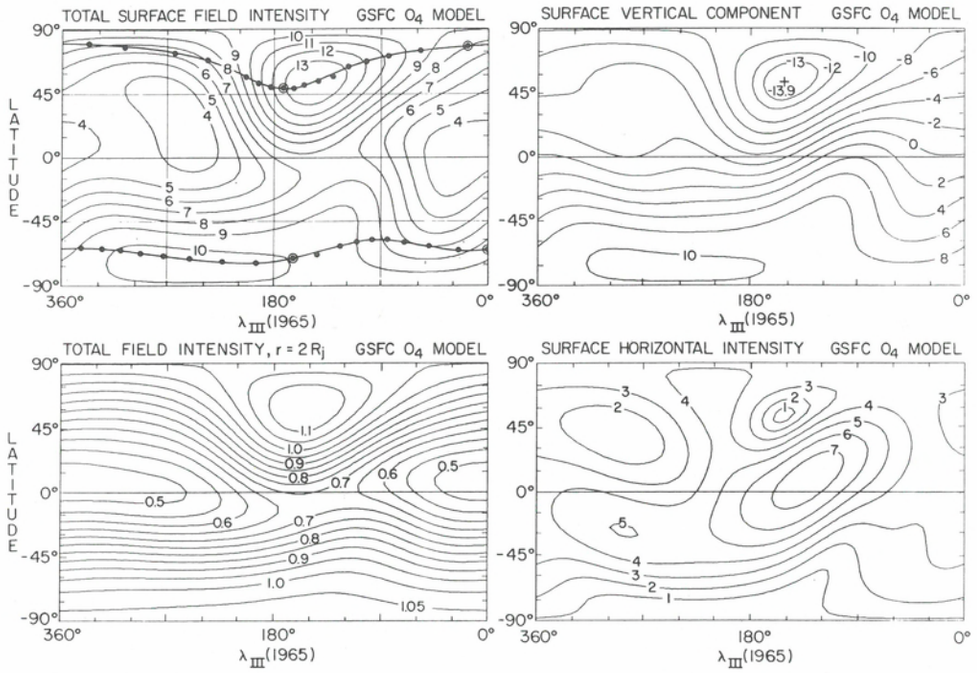

Fig. 1.1. Isocontour maps of total field intensity as predicted by the O_4 model at the surface and at 2 Jovian radii. The vertical and horizontal field intensities at the surface are also shown. Note that the dynamic flattening of 1/15.4 has been incorporated into the surface maps. Also shown in upper left panel are traces of the feet of the field line (flux tube) through Io (filled circles on solid curves).

The dip and declination angles are defined in the usual sense for Earth's case: dip = $\tan^{-1} Z/H$, where Z and H denote the local vertical (downward) and horizontal field components, respectively, and declination = $\tan^{-1} Y/X$, where X is the local field component directed towards the north and Y the local field component directed towards the east. Note that the surface maps take into account Jupiter's dynamic flattening, $f = 1/15.4$; those computed at 2 R_J assume a spherical surface. From the coefficients given in Table 1.1 and the maps shown in Figures 1.1 through 1.3 it is clear that Jupiter possesses substantial quadrupole and octupole moments which lead to a relatively complex field morphology extending to significant distances from the planet although the field is largely dipolar for distances as close as 2 R_J. On the surface the maximum field strength at the poles is asymmetrical, ~14 and 10.4 G in the north and south polar regions, respectively. The relatively large high-order terms also imply that the sources of the magnetic field, presumably in Jupiter's core, lie closer to the surface than in the case of the Earth.

A new estimate of Jupiter's planetary magnetic field has been obtained from the Voyager 1 observations. Connerney, Acuña and Ness [1982] combined an explicit model of the magnetodisc current system with a spherical harmonic model of the planetary field and obtained most of the parameters of an octupole internal field model. The resulting model fits the observations extremely well (Fig. 1.4) throughout the analysis interval ($r < 20\ R_J$) and is very similar to the octupole Pioneer 11 models. Comparing dipole parameters of the epoch 1979.2 Voyager 1 model with the epoch 1974.9 O_4 model, Connerney, Acuña, and Ness find no statistically significant change in Jupiter's dipole moment, tilt angle or longitude.

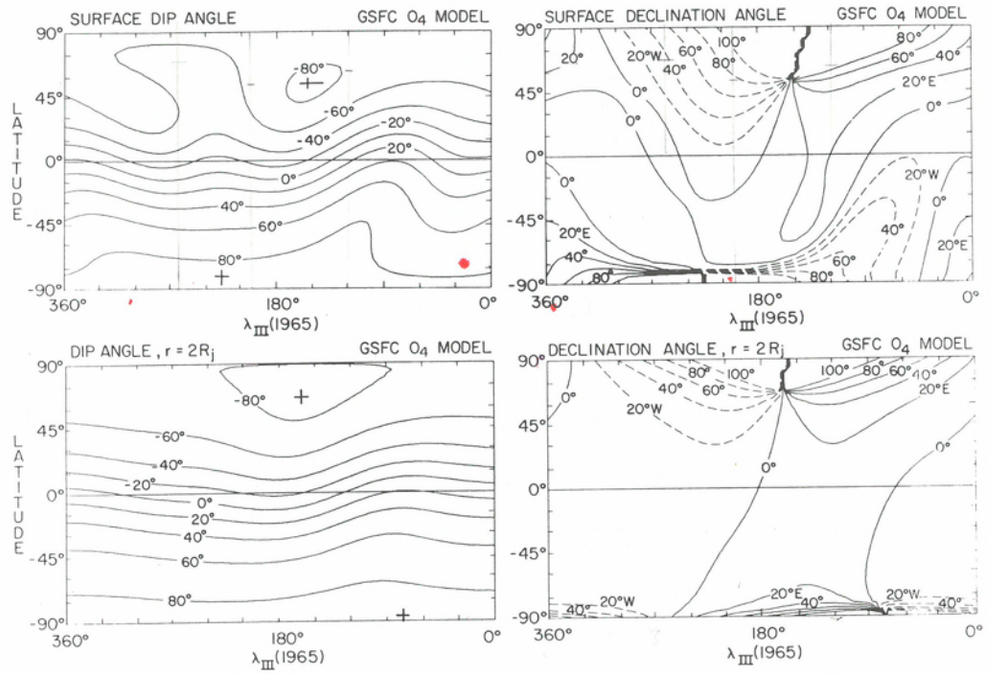

Fig. 1.2. Isocontour maps of declination and dip angles as predicted by the O_4 model for the surface and 2 Jovian radii. See text for the definition of these angles. A dynamic flattening of 1/15.4 has been incorporated into the surface maps.

Offset tilted dipole

A simplified model for the field can be obtained by fitting the data to a noncentered dipole. Alternatively, an offset, tilted dipole (OTD) representation can be derived from the quadrupole terms in the form given by Bartels [1936]. These offset, tilted dipole models of the Jovian field find application in problems that require a simple magnetic field model for computational ease and are not concerned with the detailed morphology of the field near the surface. A typical widely used offset, tilted dipole model is the D_4 model of Smith, Davis, and Jones [1976]; its characteristics are given in Table 1.3.

Table 1.3. *Characteristics of offset tilted dipole (OTD) models of the Jovian magnetic field*

Model	$\|M\|$	Tilt	λ_{III} (1965)	Offset (R_J)	δ^b	μ(1965)
D_4	4.225	10.8°	200.8°	0.101	5.1	155.6°
OTD[a]	4.35	9.5°	208.8°	0.068	−12.6°	174.2°
O_4	4.28	9.6°	201.7°	0.131	− 8.0°	148.57°
P 11(3,2)*A*	4.208	10°	198.8°	0.108	4.8°	143.07°

[a] Acuña and Ness [1976c].
[b] δ and μ are the latitude and longitude of the offset vector in System III (1965).

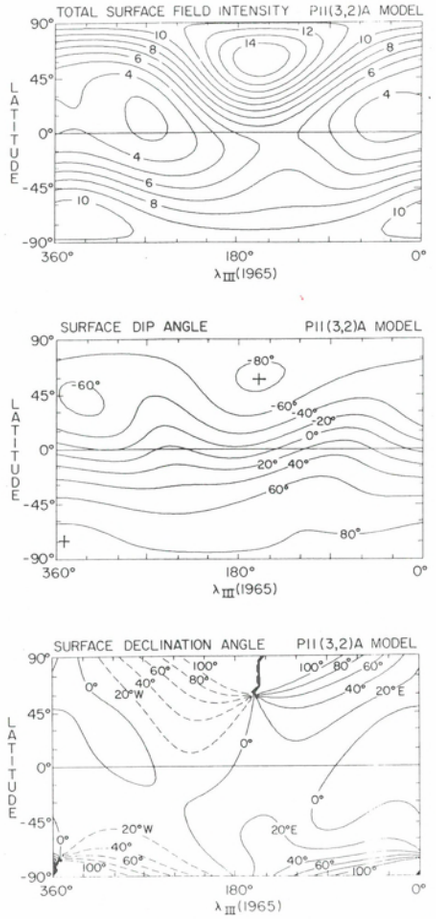

Fig. 1.3. Surface total field intensity, dip, and declination angles as predicted by the P 11(3.2)*A* model. See text for definition of the angles.

Also in the table are given the equivalent OTD models derived from the O_4 model and the P 11(3,2)*A*.

It can be argued that the OTD models represent the simplest morphological structure (dipole) associated with the planetary field. The degree of complexity is given by a measure of how far the real field deviates from this zeroth order representation. This has been illustrated in Figure 1.5 where we have plotted isointensity contours on the surface of the planet for the difference field between the O_4 and the OTD models of Acuña and Ness [1976c]. A strong quadrupolar component remains evident in this figure, indicative of a field complexity at the surface which cannot be adequately represented by OTD models.

An important point that must be kept in mind when using analytical models of planetary magnetic fields is their nonuniqueness. Magnetic field observations acquired along a flyby trajectory, for example, are insensitive to certain linear combination of parameters. This has been illustrated by the "invisible planet" constructed by Connerney [1981a] in connection with the Pioneer 11 flyby trajectory at Jupiter. This figure is reproduced in Figure 1.6 showing surface isocontour maps of Jovian model magnetic fields that would not have been detected by the magnetometers on Pioneer 11, assuming (Fig. 1.6*a*) a uniform noise distribution and (Fig. 1.6*b*) observation noise proportional to the local field magnitude.

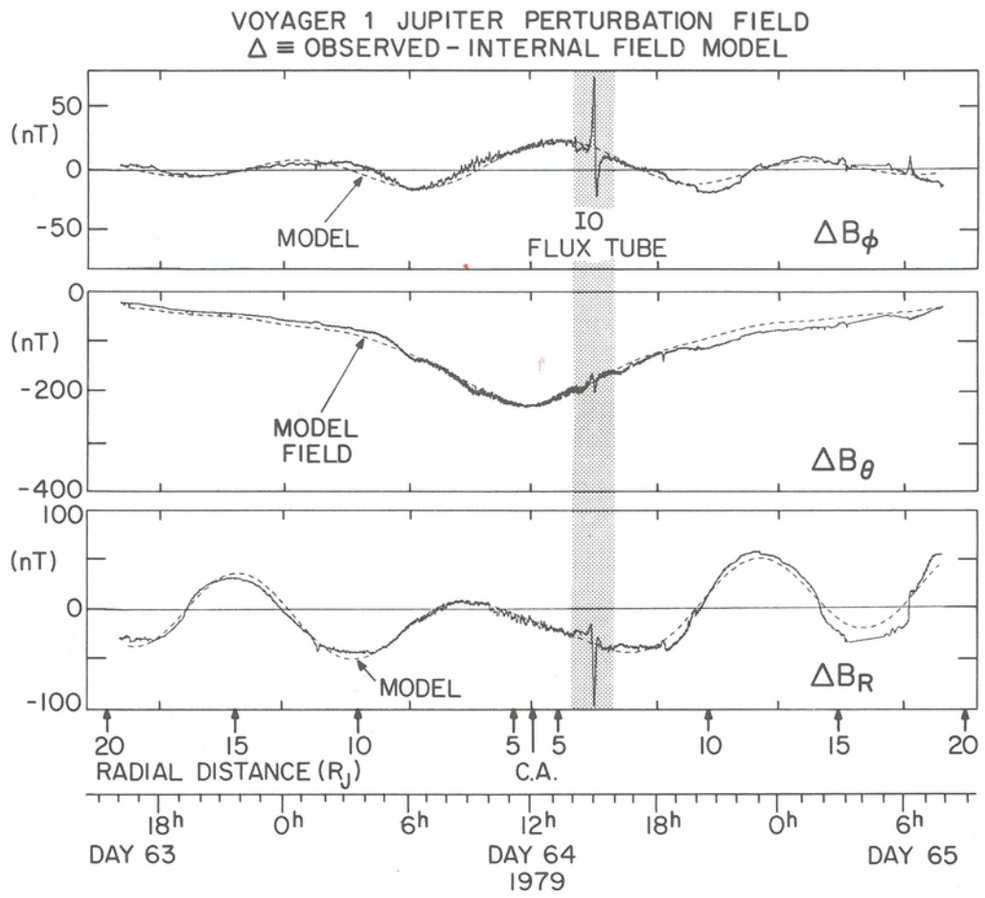

Fig. 1.4. Comparison of modeled magnetic field (dashed) with that observed for Voyager 1 (spherical coordinates are used). In this presentation the model internal field has been subtracted from the observations; the remaining model field (dashed) is due to Jupiter's magnetodisc currents. The total field at closest approach (C.A.) is ~3330 nT (from Connerney, Acuña, and Ness, 1982).

Magnetic field geometry relevant to energetic particle trapping

Energetic particles trapped in the Jovian magnetosphere serve as excellent tracers of the magnetic field morphology, since in their bounce and drift motions around the planet they trace out the magnetic field lines over a large region of space. Thus, energetic particle measurements aboard spacecraft play an important role in establishing the global characteristics of the field (see for example Van Allen et al. [1974a]), and in providing independent evidence against which the validity of the magnetic field models can be tested. The satellites in the Jovian system act to remove trapped energetic particles by absorption into their surfaces [Mead and Hess, 1973]. The observed absorption signatures and their relative locations with respect to the planet can be used effectively to infer characteristics of the magnetic field [Acuña and Ness, 1976c; Van Allen, 1976;

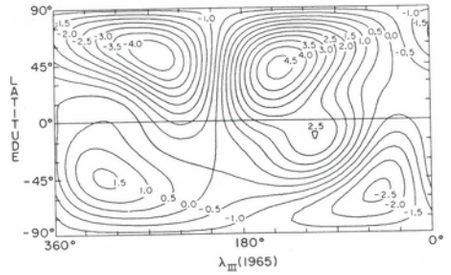

Fig. 1.5. Isocontour map of the differential in total surface field intensity computed by subtracting the OTD model of Acuña and Ness from the O_4 model. The large remaining quadrupolar and higher order contributions to the field cannot be adequately modeled by an offset, tilted dipole.

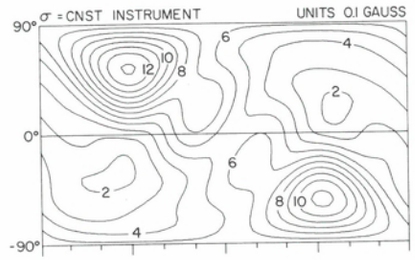

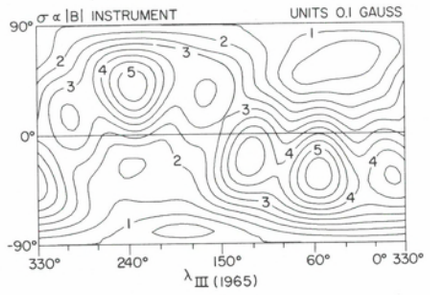

Fig. 1.6. "Invisible planet": Surface isointensity contour map of a Jovian model magnetic field that would not have been detected by a magnetometer on Pioneer 11: (a) (upper panel) assuming observations with a .005 G random noise component; (b) (lower panel) with a noise component proportional to the local field magnitude (see text). A dynamical flattening of 1/15.4 is assumed in the determination of the surface equipotential (from Connerney [1981a]).

Simpson and McKibben, 1976; Fillius, 1976]. Conversely, the magnetic field models in conjunction with observed energetic charged particle absorption effects can be used to infer the presence and properties of undetected absorbers such as unknown rings and satellites [Van Allen et al., 1980; Acuña and Ness, 1976c; Fillius, 1976].

It is important therefore to determine the adiabatic particle parameters for particle detectors aboard a given spacecraft and trajectory. For example, *L*-shells and equatorial pitch angles for charged particles incident from a given direction constitute extremely useful quantities. (For a detailed discussion of adiabatic particle motion and parameters in a planetary magnetic field the reader is directed to Roederer [1970]). An example of this type of calculation using the O_4 model is given in Figure 1.7 for the Pioneer 11 spacecraft encounter trajectory and for particles with pitch angles equal to 90° at the spacecraft. Also shown in the figure are the range of *L*-shells swept by Io and Amalthea, as predicted by several models, where absorption effects should be observed [Van Allen et al, 1974a; Fillius, Mogro-Campero, and McIlwain, 1975]. Note that the range of *L*-shells swept by these two satellites as they move around in their orbits is

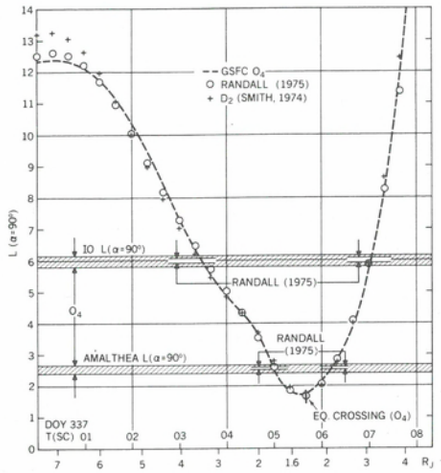

Fig. 1.7. McIlwain "*L*" parameter values computed for charged particles with 90° pitch angle at the spacecraft. The trajectory is that of Pioneer 11 at Jupiter. The shaded regions indicate the range of *L*-shells swept by the Jovian satellites Io and Amalthea, where particle absorption effects should be observed. See Van Allen [1976] for a description of the Randall (1975) model.

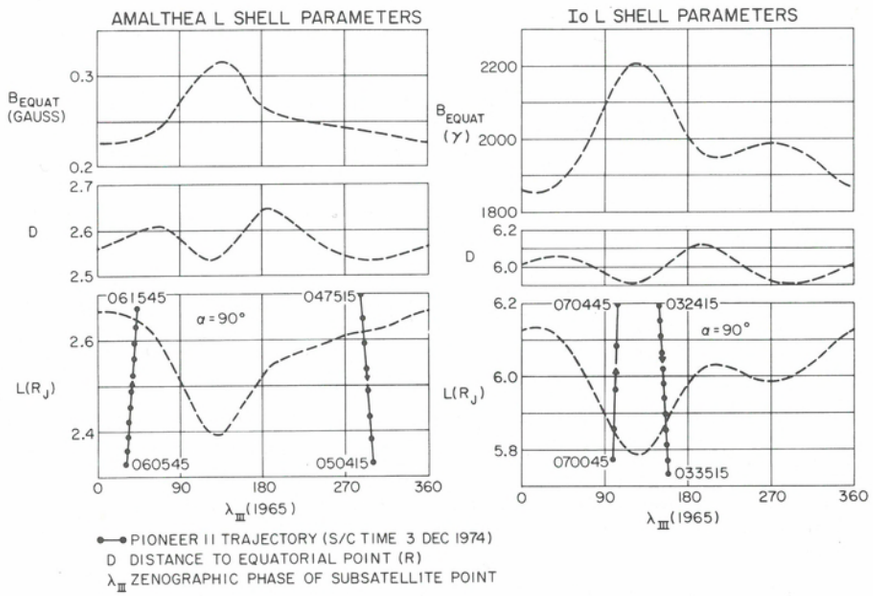

Fig. 1.8. *L*-parameter values computed for the "trajectories" (orbits) of Io and Amalthea around Jupiter. Note the large range of *L*-values which the satellites traverse around their orbits. The indicated longitude is System III (1965).

much broader for the O_4 and P 11(3,2)*A* models than predicted by dipole models [Acuña and Ness, 1976c], as illustrated in Figure 1.8. This effect becomes pronounced for satellites in the middle magnetosphere, such as Ganymede, where the field lines are stretched out radially by external currents. These effects are discussed in the next section.

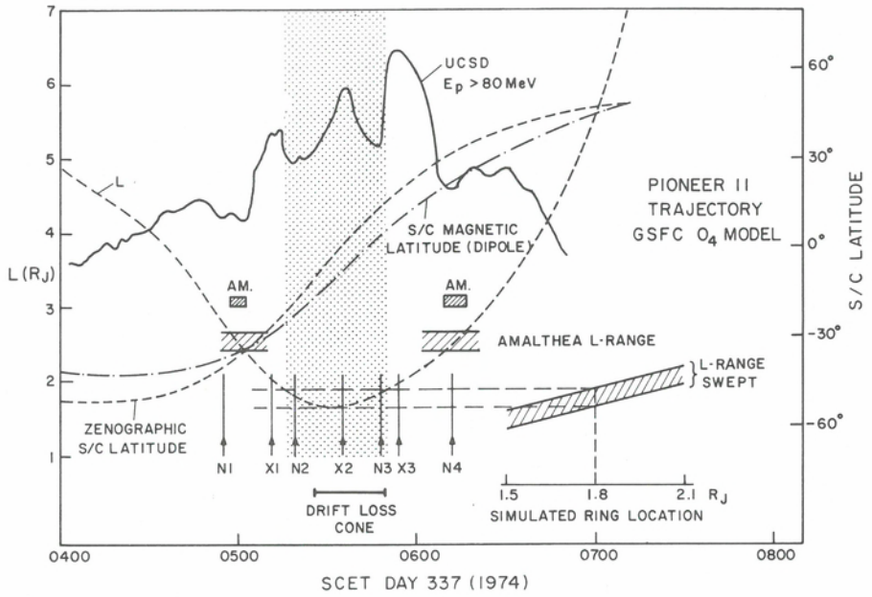

Fig. 1.9. Pioneer 11 observations of the Jovian ring. The charged particle data is that of Fillius [1976]. The L-values along the trajectory of Pioneer 11 and Amalthea were calculated using the O_4 model. A narrow ring located at 1.8 R_J provides an excellent fit to the observed absorption features N2 and N3.

One of the most interesting applications of adiabatic particle motion principles and satellite sweeping effects was the anticipation of the existence of a ring of particles around Jupiter at 1.8 R_J [Acuña and Ness, 1976c; Fillius, 1976; McLaughlin, 1980]. This is illustrated in Figure 1.9 where the Pioneer 11 spacecraft trajectory near closest approach in L-space and magnetic latitude is shown. Also shown are the energetic particle data of Fillius, Mogro-Campero, and McIlwain [1975] illustrating the existence of a multiply peaked structure in the count rate near closest approach. The two outer minima in the curve are due to absorption of energetic particles by Amalthea and correspond very closely to Amalthea's L-shell. The two inner minima are adequately explained by assuming the existence of a narrow absorber at 1.8 R_J, as indicated in the figure. This narrow ring was later observed by the Voyager 1 imaging experiment [Smith et al., 1979b]. The interpretation of the two minima being due to the presence of an absorber (ring or satellite) was considered remote since planetary rings had only been observed at Saturn [McLaughlin, 1980]. An analysis of the idealized response of energetic charged particle detectors aboard P 11 in an ambient magnetic field given by the O_4 model by Roederer, Acuña, and Ness [1977] indicated that the absorption signature could also be associated with geometric effects due to the intersection of the drift loss cone [Roederer, 1970] with the angular response of the detectors. This effect is indeed operative close to the planet but absorption by the ring material is the dominant loss mechanism.

It is also instructive to compute the configuration of the intersections of particle drift shells with the planetary ionosphere in order to locate areas where the mirror points for the trapped particles are low enough in altitude to interact strongly with the atmosphere–ionosphere. Constant L contours computed for the O_4 model are shown in

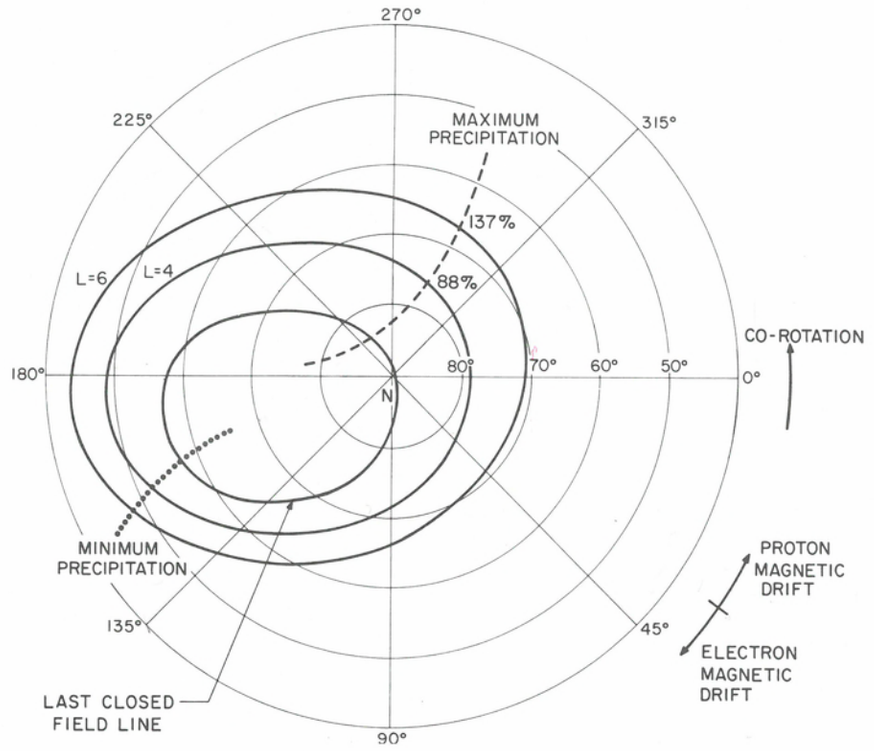

Fig. 1.10. L = constant drift shell intersections with the planetary ionosphere in the northern hemisphere of Jupiter. Dashed and dotted lines represent zones of maximum and minimum precipitation flux. The percentage values represent the relative variation of the precipitation function between minimum and maximum along a given L = const. contour for each hemisphere. [Roederer, Acuña, and Ness, 1977; Connerney, Acuña and Ness, 1981].

Figure 1.10 and 1.11 in Jovigraphic coordinates for the northern and southern hemisphere, respectively [Roederer, Acuña, and Ness, 1977]. Also included in this figure is the contour of last closed field lines as predicted by the model of Connerney, Acuña and Ness [1981] which is discussed in the next section. What is important in Figures 1.10 and 1.11 is the expected location of maximum and minimum particle precipitation flux along a given contour because these regions, in principle, could play an important role in the generation of decametric emissions from Jupiter and their control by Io [Dessler and Hill, 1979 and references therein]. The discovery and observations of the Io plasma torus [Kupo, Mekler, and Evitar, 1976; Broadfoot et al., 1979] have changed significantly this point of view, and although the precipitating particles are probably still responsible for the Io-independent emissions, their role is not completely understood. An attempt to correlate the precipitation regions with the decametric source regions as a function of central meridian longitude has been carried out by Roederer, Acuña, and Ness [1977] (see also Chap. 7).

Although our understanding of the emission mechanisms and source geometry is incomplete, the magnetic field models provide further insight into the decametric and decimetric emission phenomena. Synchrotron emission by relativistic electrons mirror-

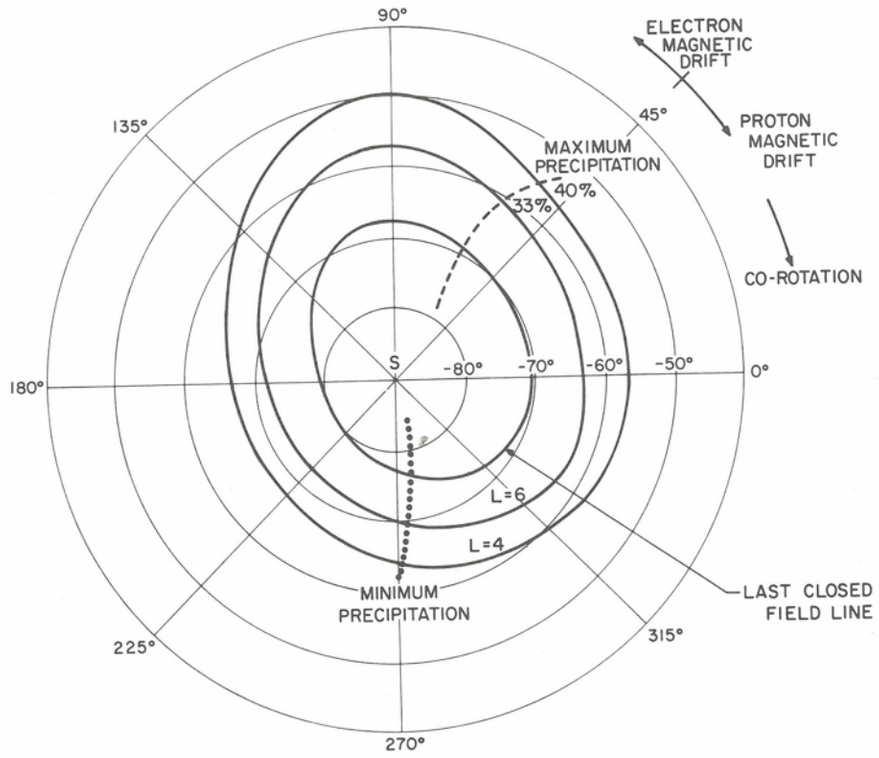

Fig. 1.11. Same as Figure 1.10, but for the southern hemisphere of Jupiter.

ing near the magnetic equatorial plane is the source of decimetric radiation. Acuña and Ness [1976a,b] first used the O_4 model to compute the charged particle equator at different radial distances from the planet, and the results of this calculation are shown in Figure 1.12 for $r = 1, 2, 4$, and 6 R_J. The curves clearly illustrate the nonsinusoidal character of the magnetic equator or, equivalently, the "warping" of the decimetric emission region away from a simple flat disc. This explains the observed polarization characteristics at Earth [Carr and Gulkis, 1969; Berge and Gulkis, 1976; see also Chap. 3]. These preliminary studies have been extended by Smith and Gulkis [1979] and particularly by de Pater [1980b] to include the P 11(3,2)*A* model and realistic pitch angle distribution functions for the electrons. These studies confirm the good agreement between the decimetric observations and the analytical models of the magnetic field.

The Io flux tube

Theoretical explanations of the enigmatic control of Jupiter's decametric emissions by the satellite Io are based on a strong electrodynamic interaction with the corotating Jovian magnetosphere, leading to field-aligned (Birkeland) currents connecting Io with the Jovian ionosphere [Piddington and Drake, 1968; Goldreich and Lynden-Bell, 1969; Carr and Desch, 1976]. The interaction model is illustrated in Figure 1.13. The corotational electric field developed by the relative motion between Io and the magnetic field lines swept past the satellite (~57

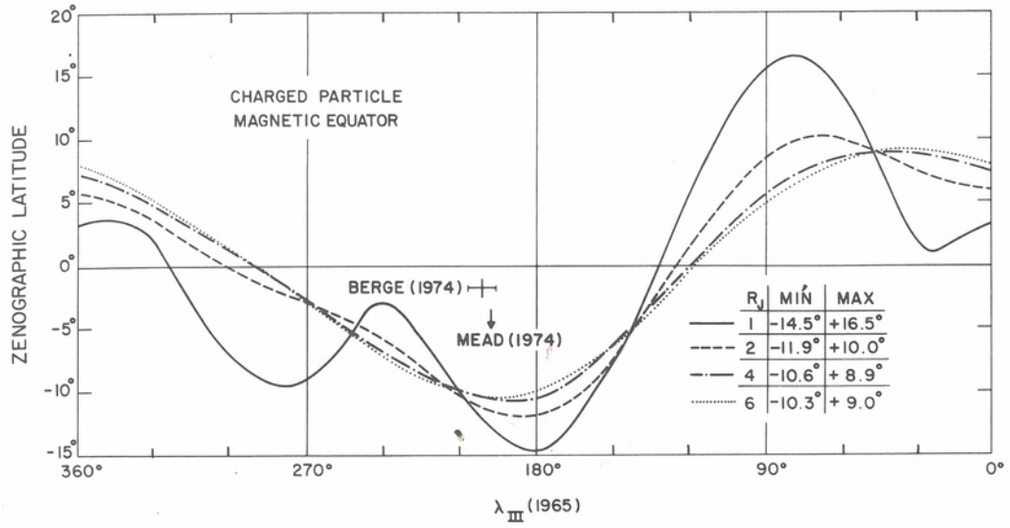

Fig. 1.12. Energetic charged particle magnetic equator ($|B|$ = min. along field line) computed from the O_4 model at several radial distances. Notice the deviation from a simple sinusoid predicted by the model, which is in good agreement with decimetric radio observations [Smith and Gulkis, 1979; de Pater, 1980b].

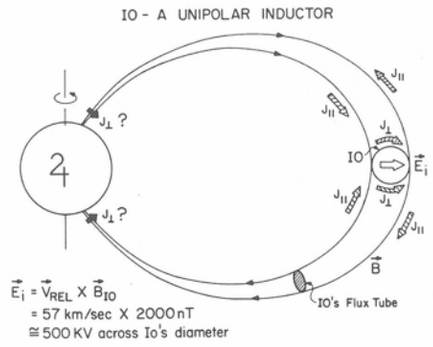

Fig. 1.13. Io as a unipolar inductor. Schematic representation of the induced current system flowing approximately parallel to the field lines in the flux tube linking Io to the Jovian ionosphere/atmosphere. The circuit is closed at the extremes by currents flowing in the Jovian ionosphere and in the ionosphere and/or interior of Io. A power of approximately 10^{12} W is dissipated in the system.

km/s) induces a potential difference of approximately 500 kV between the outer and inner faces of this satellite. This potential causes currents to flow from Io toward the Jovian ionosphere, both northward and southward, along the outer portion of the magnetic flux tube linking the satellite to the ionosphere. Return currents flow along the inner portions of the flux tube towards Io. In this simple model, the circuit is closed through the Jovian ionosphere, Ionian ionosphere and/or the interior of the satellite. The term "unipolar inductor" is applied to this type of interaction between a satellite and a planetary magnetosphere. The presence of the Io torus (i.e., a dense plasma) introduces additional plasma-inertial effects, and hence the simple model described above has to be expanded to include these effects leading to the concept of an "Alfvén current tube" as explained further below. Direct measurements of the perturbation magnetic fields due to the Io induced current system were obtained by the magnetic field experiment on Voyager 1 on 5 March 1979 when it passed within 20,500 km south of Io [Ness et al., 1979a; Acuña, Neubauer, and Ness, 1981].

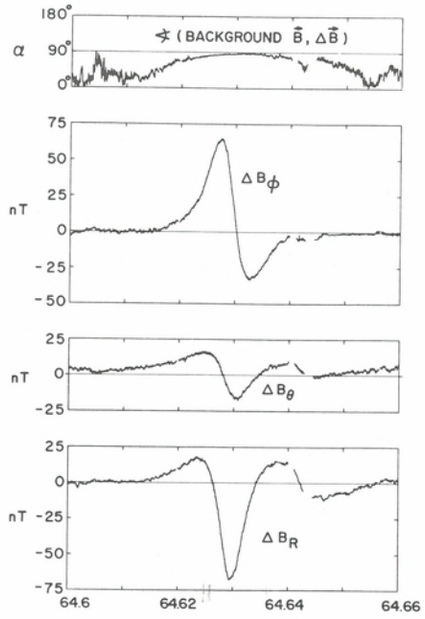

Fig. 1.14. Perturbation magnetic field associated with the Io current system as detected by Voyager 1. In addition to the three orthogonal components in spherical coordinates, the angle between the background field and perturbation has been computed and is shown in the upper panel. The abscissa is the decimal day (SCET).

The Voyager 1 spacecraft encounter trajectory had been designed specifically to provide a passage at close range to the satellite through the south magnetic flux tube depicted in Figure 1.13. The geometrical position of the flux tube had been calculated on the basis of analytical models of the field without taking into account possible distortions introduced by the system of currents. During the time interval associated with the anticipated Io flux tube passage, the magnetic field experiment detected significant perturbations superimposed on the much larger background planetary field. The observations are shown in Figure 1.14 where the differences between a local model background field and the measurements are illustrated in Jupiter centered, spherical polar coordinates. The top panel in the figure shows that the angle between the perturbation field and the background field approached 90° during this interval, indicating the transverse nature (i.e., due to field aligned currents) of the perturbation. A preliminary report and analysis of quick look data was given by Ness et al. [1979a], which did not include the plasma inertial effects introduced by the presence of the Io plasma torus [Broadfoot et al., 1979; Bridge et al., 1979a]. The presence of the plasma leads to a "slowing down" of the magnetic field lines being swept past the satellite or, equivalently, to the generation of an Alfvén wave that propagates away from Io approximately parallel to the ambient field. The plasma density in the torus [Warwick et al., 1979a; Bridge et al., 1979a; Bagenal, Sullivan, and Siscoe, 1980] is such that plasma flow past Io is sub-Alfvénic, and hence no shock forms in front of the object. The interaction geometry is illustrated in Figure 1.15 for an Alfvén Mach number of 0.25 and a sonic Mach number of 1.

The general description of this type of interaction in terms of Alfvén waves propagating away from a satellite was first given by Drell, Foley, and Ruderman [1965]. Neubauer [1980] extended Drell's analysis to the nonlinear case and described Io's interaction with the Jovian magnetosphere as a nonlinear standing Alfvén current system (see also Goertz [1980a]). A detailed analysis of the Voyager 1 observations in terms of this Alfvén current system has been given by Acuña, Neubauer, and Ness

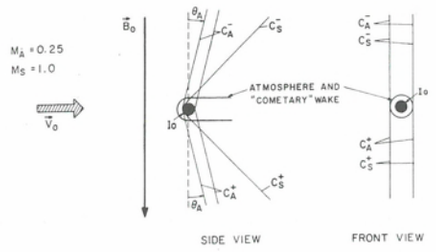

Fig. 1.15. Example of linear Alfvén and slow wave characteristics for $M_A = 0.25$ and sonic Mach number $M_s = 1$. Strong Alfvénic disturbances are expected to issue from Io and its vicinity along the appropriate tube of Alfvén characteristics [from Neubauer, 1980].

[1981] and leads to an estimate of 2.8×10^6 A for the currents flowing in the Alfvén current tube. This value for the current is strongly dependent upon the geometry assumed for the current tube due to the nonuniqueness of the model assumed to represent the observations. The smallest total current consistent with the Voyager 1 observations is obtained for a current sheet located just inside the flyby trajectory as seen from Io. Its value is given by $I_{min} = 6 \times 10^5$ A [Acuña, Neubauer, and Ness, 1981]. The total power dissipated in the system amounts to 1.8×10^{12} W. For additional discussions concerning alternative Alfvén current tube models the reader is referred to Southwood et al. [1980]. In addition to the magnetic field perturbations detected by the magnetometer experiment on Voyager 1, the plasma experiment detected plasma velocity perturbations consistent with the Alfvén standing wave system described above [Belcher et al., 1981; Goertz, 1980a, and see Chap. 3]. An important development associated with the Alfvén current system and the Io torus has been the work of Gurnett and Goertz [1981] concerning the generation of discrete decametric arcs [Warwick et al., 1979a,b] and the control of decametric emissions by Io. In this model the discrete arc structure is explained as due to multiple reflections of the Alfvén waves at the torus boundaries and Jovian ionosphere. The position of Io within the torus determines the degree of interaction with the atmosphere/ionosphere system (see Chap. 3).

1.3. The middle magnetosphere

We are concerned in this section with a description of the magnetic field in that region of space where the Jovian internal field is adequately represented by a tilted dipole and where the magnetic field of the magnetopause currents and tail currents is small. In this region the field morphology is dominated by the field of external currents in the Jovian magnetosphere, predominantly by the equatorial azimuthal currents of the magnetodisc. Various authors have defined the radial extent of this region to suit a particular application. Van Allen et al. [1974a] and Smith, Davis, and Jones [1976] chose an inner radius of 20 R_J, while Goertz [1976a, 1979] prefers $10R_J$. The outer radius is often assumed to be 30 R_J [Goertz, 1976a] or variable, that is, extending to within $15R_J$ of the magnetopause [Smith, Davis, and Jones, 1976]. Our definition of the extent of the middle magnetosphere is motivated by the observed magnetic field morphology and the extent of the equatorial azimuthal current system established by Voyager observations [Ness et al., 1979a,b; Connerney, Acuña and Ness, 1981]. These observations demonstrate that the equatorial currents extend inward towards Jupiter at least to the orbit of Io, at ~ 6 R_J. Earlier estimates of the inner edge of the current sheet range from ~ 30 R_J [Smith, Davis, and Jones, 1976] to 17 R_J [Engle and Beard, 1980; Gleeson and Axford, 1976]. Our choice of ~ 6 R_J as the inner edge of the middle magnetosphere thus leads conveniently to a current-free (curl-free) inner magnetosphere. Although the sheet currents contribute only a fraction of the total field at 6 R_J, the

presence of a near equatorial radial component has significant consequences for charged particle motion and field line morphology. Thus, an adequate description of the field for $r > 6\ R_J$ requires consideration of the magnetodisc current system.

We confine our discussion to the in situ magnetic field observations and models of the Jovian magnetosphere based upon these observations, excluding theoretical models of a rotating magnetodisc [e.g., Gledhill, 1967] and self-consistent magnetic field/plasma models [e.g., Goldstein, 1977]. We do not discuss the magnetic anomaly model [Dessler and Hill, 1975; Dessler and Vasyliunas, 1979; Vasyliunas and Dessler, 1981 and Chap. 10], where correlated particle intensity maxima and magnetic field minima are related to a surface magnetic field anomaly rather than the existence of an annular current sheet. Voyager observations of two minima in the magnetic field every 10 hr [Ness et al., 1979a,b] and charged particle observations [Bridge et al., 1979a,b] require an interpretation of these data based on local currents (i.e., magnetodisc currents). Therefore, we will consider only the disc models. See Chapter 10 for a discussion of the magnetic anomaly model.

Earlier studies

One of the most distinguishing characteristics of the Jovian magnetosphere revealed by the Pioneer 10 and 11 (P 10 and P 11) encounters in 1973 and 1974 was the marked distortion of the equatorial magnetic field morphology and associated energetic particle confinement. The pervasive 10-hr periodicity in the fluxes of energetic particles [Van Allen et al., 1974a] and magnetic field perturbations [Smith et al., 1975] particularly evident in the Pioneer 10 observations was identified with the repeated encounter of the spacecraft with an immense and relatively thin annular current sheet. The misalignment of the axis of the annular current sheet and the Jovian axis of rotation results in the periodic motion of the sheet past an observer fixed near the equatorial plane. Azimuthal (eastward) currents flowing in the disc contribute a radial field component to the ambient (nearly dipolar) field of internal origin, a contribution that reverses sign through the sheet, stretching field lines radially outward along the plane of the current sheet. Thus, the middle magnetosphere can aptly be regarded as the transition from a dipolar magnetospheric configuration to the disclike geometry of the "magnetodisc." Early models placed the current disc in the magnetic equatorial plane and suggested azimuthal symmetry about the magnetic dipole axis [Van Allen et al., 1974a] tilted $\sim 10°$ with respect to the rotation axis. Hill, Dessler, and Michel [1974], Smith et al. [1975], and Smith, Davis, and Jones [1976] advocated a warping of the current sheet toward the rotational equator for $R \gtrsim 20\ R_J$, reflecting the action of centrifugal forces on the corotating plasma [Hill, Dessler, and Michel, 1974], but Goertz et al. [1976] and Goertz [1979] argued that the disc deviated only slightly from the magnetic equator to at least 90 R_J. The magnetic anomaly advocates [Vasyliunas and Dessler, 1981] propose a current sheet that remains in the equatorial plane but exhibits longitudinal asymmetries related to magnetic anomaly effects.

Voyagers 1 and 2 (V 1 and V 2) traversed the Jovian magnetosphere outbound at 0420 and 0300 local time, respectively, supplementing the P 10 and P 11 outbound observations at 0500 and 1200 local time. Voyager investigations provided additional direct observations of the magnetic field [Ness et al., 1979a,b], as well as measurements of particles and plasmas not obtainable by P 10 and P 11 [Bridge et al., 1979a,b; Krimigis et al., 1979a,b; and Warwick et al., 1979a,b]. In addition, the V 1 and V 2 spacecraft trajectories were more favorable for observations of the azimuthal current sheet (in or near the magnetic equator), because the Voyager spacecraft approached

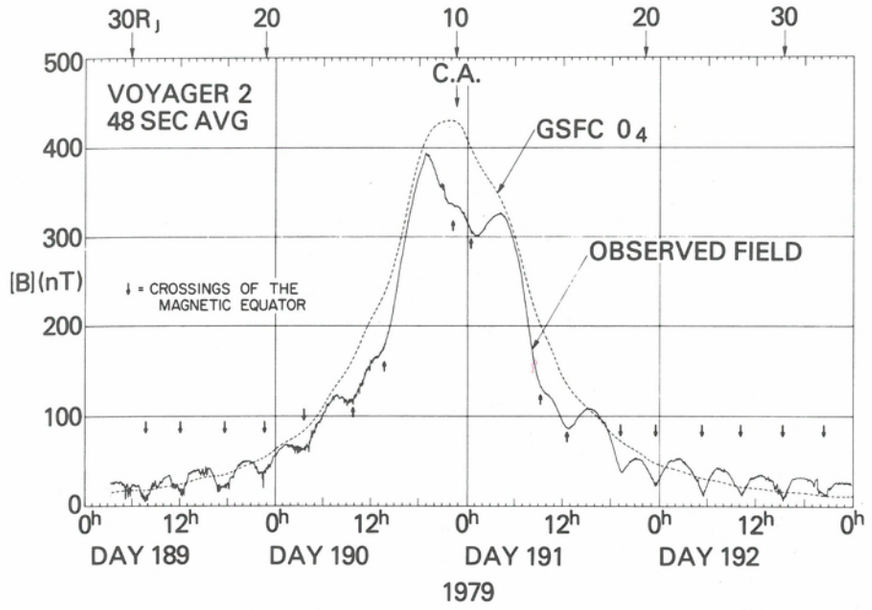

Fig. 1.16. Magnetic field magnitude observed by Voyager 2 during the encounter. The dashed curve is the model intrinsic magnetic field of Jupiter assuming the O_4 internal field model of Acuña and Ness [1976c], obtained from Pioneer 11 observations. Field magnitude minima occur at crossings of the magnetic equator, where the field of the azimuthal current sheet is antiparallel to Jupiter's (dipolar) intrinsic magnetic field. At larger radial distances, just above the disc currents (where the radial field component of the disc currents reaches a maximum), the (vector summed) total field magnitude exceeds the intrinsic field.

(and exited) closer to the Jovigraphic equator than the Pioneers. The Voyagers passed through the current sheet twice each planetary rotation, at times completely traversing the current disc. In contrast, the Pioneer inbound trajectories, in particular the P 10 approach at $\sim 5°$ southerly Jovigraphic latitudes, brought these spacecraft close to the center of the current sheet (near the magnetic equator) and produced only one encounter with the sheet for each planetary rotation. P 10 outbound was similar, and P 11 exited at middle or high northerly latitudes, missing the sheet entirely. Thus, the Voyager encounters were instrumental in clarifying the observations of the magnetodisc obtained along the rather singular P 10 trajectory. Although these observations enabled a more complete description of the distant Jovian magnetotail [Behannon, Burlaga, and Ness, 1981; see also next section], it is important to realized that a major portion of the voluminous Jovian magnetosphere, for example, from 1200 LT to 0300 LT, remains unexplored.

Observations

The periodic magnetic field perturbations typical of each of the spacecraft traversals of the Jovian magnetosphere are illustrated in Figure 1.16 for the V 2 encounter. In this figure the observed magnetic field magnitude is compared with that predicted by the GSFC O_4 internal Jovian field model, a 15 coefficient, spherical harmonic expansion derived from P 11 observations [Acuña and Ness, 1976c]. The now familiar field

magnitude depressions, coincident with crossings of the magnetic equator, are evident, as well as systematic enhancement of the field magnitude at larger radial distances whenever the spacecraft emerges from the current sheet. The P 10 and P 11 observations demonstrate a similar decrease in the field magnitude as the spacecraft nears the center of the azimuthal current sheet, although these field depressions occur only once each planetary rotation because of the trajectory constraints discussed earlier [Smith et al., 1975; Smith, Davis, and Jones, 1976].

A very useful and revealing presentation of the magnetospheric magnetic field data for studies of magnetic fields of external origin is that of a perturbation magnetic field plot. The perturbation field $\Delta\mathbf{B}$ is the difference between the observed magnetic field at any position and the predicted field of internal origin. In the present example, the GSFC O_4 model of the internal Jovian magnetic field is used. The perturbation computed field is increasingly sensitive to the model internal field at radial distances $<6\ R_J$ where inaccuracies in predicting the rapidly increasing internal field become important. Consequently, we will concentrate at present on the observations at radial distances $>6\ R_J$.

Examination of the perturbation field in spherical (1965 System III) coordinates for the Voyager 1 encounter (Fig. 1.16) reveals:

1. a slowly varying theta component ΔB_θ increasing in magnitude approaching Jupiter and antiparallel with the internal (nearly dipolar) field;
2. a small azimuthal (phi) component ΔB_ϕ;
3. a radial field component ΔB_r exhibiting a definite 10-hr periodicity, changing sign twice every 10 hours, and increasing in magnitude (more slowly than the theta component) with decreasing radial distance, and
4. a perturbation field direction, as determined by the angle between $\Delta\mathbf{B}$ and $\mathbf{B}_0$ which periodically varies, as the planet rotates, from being almost perpendicular to being almost antiparallel to the internal field direction.

This perturbation field due to the current sheet possesses the solenoidal field geometry appropriate to a system of azimuthal equatorial currents. At small radial distances the perturbation field is largely vertical and antiparallel to the internal field. At the magnetic equator, the radial field is zero, and the total field magnitude (e.g., Fig. 1.16) reaches a minimum. Above the magnetic equator, the radial field is positive outward and below the equator, inward.

Comparison of the perturbation magnetic field (Fig. 1.17) and the spacecraft trajectory in magnetic equatorial coordinates (Fig. 1.18) suggests that the plane of symmetry of the current system lies in or near the magnetic equator. The important features in the perturbation field plot (Fig. 1.17) can be understood by application of Ampere's Law to a narrow circuit centered about the plane of symmetry of the sheet (Fig. 1.19). The contribution of $\int \mathbf{B} \cdot \mathbf{dL}$ along the vertical segments of the circuit is negligible because the vertical field component varies little over the width Δr (Fig. 1.17). Only the radial field component, B_r, which changes sign above and below the plane of symmetry of the sheet, contributes to the integral. By Ampere's Law,

$$\int \mathbf{B} \cdot \mathbf{dL} = \mu_0 I_{\text{encl}}$$

The radial component of the field is a local measure of the azimuthal current density. Thus, the current density at $r = 10\ R_J$, assuming a total sheet thickness of $5R_J$, is easily estimated from the magnitude of the radial field component above the sheet (~ 50 nT) to be ~ 0.224 mA/km^2 ($\sim 1.13 \times 10^6\ A/R_J$). In Figure 1.17, we note that the

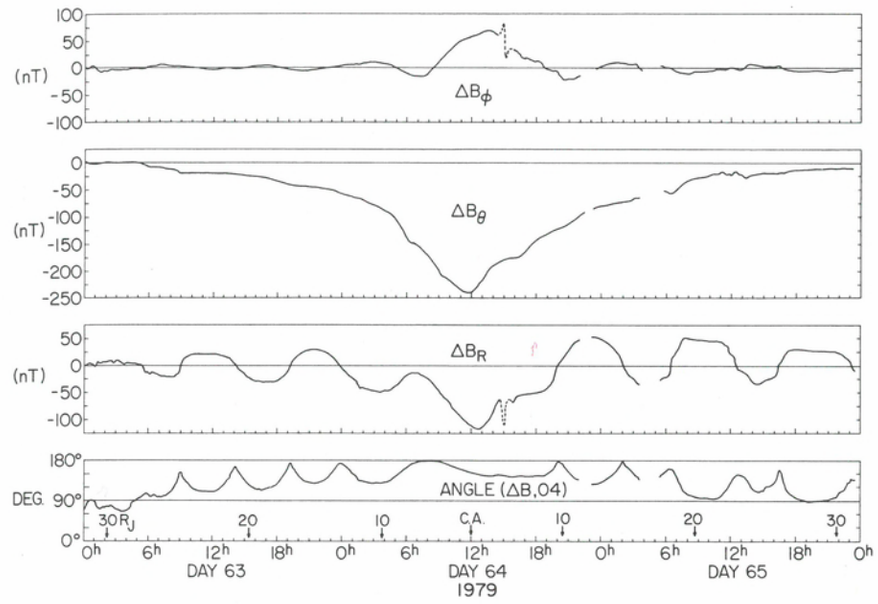

Fig. 1.17. Perturbation magnetic field $\Delta\mathbf{B}$ observed by Voyager 1 during passage through the Jovian magnetosphere for $R < 30\ R_J$. The reference field used is the GSFC O_4 model of Acuña and Ness [1976c]. Spherical coordinates are used. The angle between the perturbation field and the reference field is shown in the bottom panel.

radial field increases linearly with increasing z from zero at $z = 0$ to a maximum B_r just above the sheet (for example, V 1 outbound at approximately 0730 on day 65). Above the sheet, exterior to the current-carrying region, the radial field varies slowly with z, as is appropriate for a two-dimensional current geometry. The spacecraft reenters the current sheet at approximately hour 1120 at greater radial distance where the radial field above the sheet is slightly diminished, and again approaches zero at the magnetic equator. Note that the transition from the current sheet to the current-free region is both well-defined and unambiguous. The decrease in B_r just above the sheet from 0730 on day 65 to 2200 on day 65 is clear evidence for a decrease in the current density with increasing r, very nearly approaching a $1/r$ dependence in this region of the magnetodisc. The theta component of the perturbation field is likewise consistent with the assumed solenoidal field geometry, and the phi component is understood as a consequence of the misalignment of the symmetry plane of the annular current sheet and the System III coordinate system.

Magnetodisc magnetic field models

Magnetic field observations are obtained only along spacecraft trajectories through the Jovian magnetosphere, but we would like to have a description of the magnetic field throughout the entire magnetosphere. The difficult task of reconstructing the Jovian magnetosphere from the data obtained during the Pioneer and Voyager passes through it can and has been approached in several different ways. Engle and Beard [1980] and Beard and Jackson [1976], concerned primarily with the overall configuration of the Jovian magnetosphere and in particular the magnetopause surface shape, assumed an

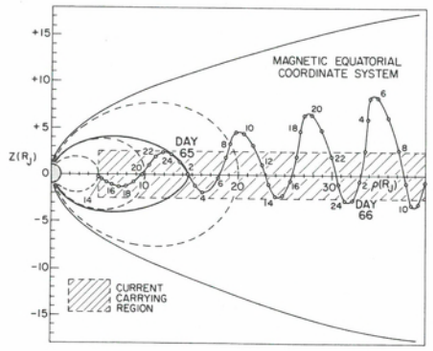

Fig. 1.18. Trajectory of Voyager 1 spacecraft in 1979 in magnetic latitude and radial distance. The location of the Connerney, Acuña, and Ness [1981] model azimuthal current sheet is shown in cross section. The near-equatorial trajectory of Voyager 2 is similar.

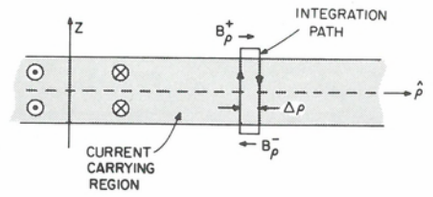

Fig. 1.19. Model of the azimuthal current sheet and appropriate ampere's circuit. The radial magnetic field component is a local measure of azimuthal current density.

infinitesimally thin equatorial current sheet and an internal dipole field, and computed this surface by equating the solar wind plasma and magnetospheric magnetic pressures. These models are not intended as detailed fits to the observations, but rather are constructed to be qualitatively consistent with the observed P 10 magnetopause crossings. They use assumed models of the equatorial current sheet. Barish and Smith [1975] confined their distended disclike model field to a spherical surface in order to approximate the blunt dayside magnetopause observed by P 10 [Smith et al., 1975]. Each of these models utilized, in addition to the available magnetic field observations, a physical constraint to shape the distant field morphology.

The more quantitative models of Goertz et al. [1976] and Connerney, Acuña and Ness [1981] are examples of two dissimilar approaches to magnetospheric modeling. The versatile Euler potential method (e.g., Stern [1970, 1976]), exemplified by the model of Goertz et al. [1976], is a mathematical representation of the magnetic field based on a description of the field morphology. Functions appropriate to the observed or assumed field line geometry are selected, and adjustable parameters are chosen to minimize the differences between the computed and observed field along the trajectory. The magnetic field at points not on the trajectory is obtained by extrapolation. In contrast, the magnetospheric magnetic field model of Connerney, Acuña, and Ness [1981] is derived from a mathematically tractable current distribution inferred from the observations. Adjustable parameters directly related to currents in the model Jovian magnetosphere are selected to minimize the differences between the modeled and observed fields along the trajectories. The magnetic field elsewhere is computed directly from the model current distribution. The distinction between these two approaches is essentially the following: in the Euler potential method, one chooses simple functions to fit the field line geometry, and accepts whatever current distribution is implied by the representation chosen. In the source modeling method, one chooses a physically reasonable current distribution, and accepts the limitations imposed by mathematical tractability and the probability of a mathematically more complex field-line description.

Euler potential models

In the Euler potential representation, the divergence-free vector magnetic field **B** is expressed as

$$\mathbf{B} = \nabla f \times \nabla g$$

where the functions f and g are scalar functions of position known as Euler potentials. Surfaces of constant f and g are everywhere tangent to **B**, because

$$\mathbf{B} \cdot \nabla f = 0$$

and

$$\mathbf{B} \cdot \nabla g = 0$$

Lines along which the surfaces f = constant and g = constant intersect are thus field lines. Stern [1976] describes the properties of Euler potentials and presents illustrative examples of their use in magnetospheric modeling.

The approximate magnetospheric model of Barish and Smith [1975] was designed to confine field lines to a sphere of radius $r = 100\ R_J$ and yield an equatorial field magnitude proportional to $1/r^2$ for $r \gtrsim 20R_J$. They used the Euler potentials

$$f = M\alpha$$

$$g = \phi$$

where M is a scale factor and α is given by

$$\alpha^6 - \frac{\alpha^5 \sin^2\theta}{r} + \frac{\ln(.01\ r)\sin^2\theta}{7.7 \times 10^{11}(\cos^2\theta + .008)} = 0$$

in a spherical coordinate system with θ denoting colatitude, ϕ the usual azimuth angle, and lengths in units of R_J. The field lines in this model do not deviate from meridional planes. The adjustable parameters were chosen to produce a field magnitude along the P 10 inbound trajectory similar to that reported by Smith et al. [1975]. The model is intended for use in the dayside magnetosphere at low latitudes.

Goertz et al. [1976] chose the functions

$$f = M\frac{\rho^2}{(\rho^2 + z^2)^{3/2}} + \frac{b_0}{(\rho^2 + z^2)^{0.7}}[\log\cosh(z) + 10]$$

and

$$g = \phi + 175(e^{\rho/500} - 1)$$

in a cylindrical coordinate system with z aligned with the magnetic dipole axis and ρ in the magnetic equatorial plane, with $M = 4GR_J^3$, $b_0 = 9 \times 10^{-2}$ G, and units of length are expressed in R_J. In this model the field lines lie in azimuthally warped surfaces given by g = constant, reproducing the spiral configuration inferred by Smith et al. [1975] from P 10 outbound observations. The agreement between the observed and computed field magnitudes along the outbound P 10 trajectory is quite good for $r \gtrsim 20R_J$, where the model is applicable. Jones, Melville, and Blake [1980] have offered two additional Euler potential models that are very similar to the Goertz et al. [1976] model.

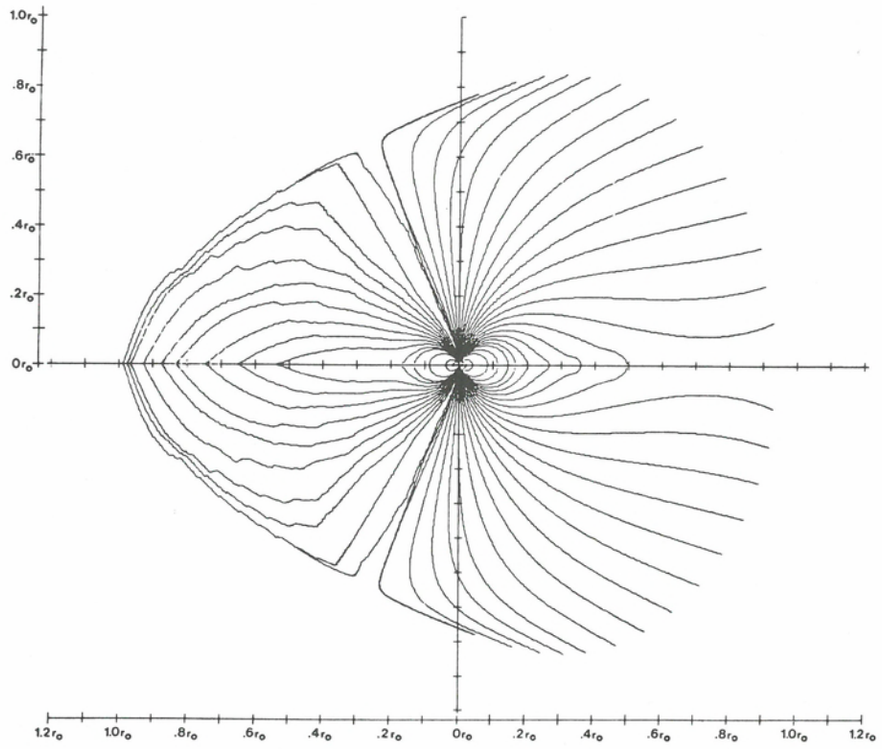

Fig. 1.20. The model Jovian magnetosphere of Engle and Beard [1980].

Source models

The only models to include the Jovian magnetopause surface currents and shape are the models of Beard and Jackson [1976] and Engle and Beard [1980]. The latter is a more complete version of the former and we will confine our discussion to it. Engle and Beard [1980] assumed an infinitesimally thin equatorial current sheet carrying an azimuthal current proportional to $1/r^{1.7}$ between $r = 18R_J$ and $r = 100\ R_J$. The choice of current sheet is intended only to be qualitatively consistent with the P 10 observations and is not the result of a fit to the observations. The resulting field morphology, consisting of contributions from the internal dipole, equatorial current sheet, and magnetopause currents, is illustrated in the noon–midnight meridian plane in Figure 1.20. The magnetopause surface is considerably flattened due to the geometry of the current sheet as compared with the magnetopause formed about a dipolar internal field. The computation of the magnetic field of the current sheet in this model is unwieldy, but the paper by Engle and Beard contains ample graphical presentations of the variations of their modeled field across the magnetosphere. They also have expressed the modeled field due to magnetopause currents as a 65 coefficient spherical harmonic expansion, which they argue is relatively insensitive to the details of the equatorial current sheet. The reader is referred to the paper by Engle and Beard [1980] for details of the computations and lists of model coefficients.

Connerney, Acuña, and Ness [1981] model the Jovian magnetosphere for $r \lesssim 30\ R_J$, where the field due to magnetopause currents is negligible. The model consists of a finite thickness ($5\ R_J$) annular current sheet with an azimuthal current density

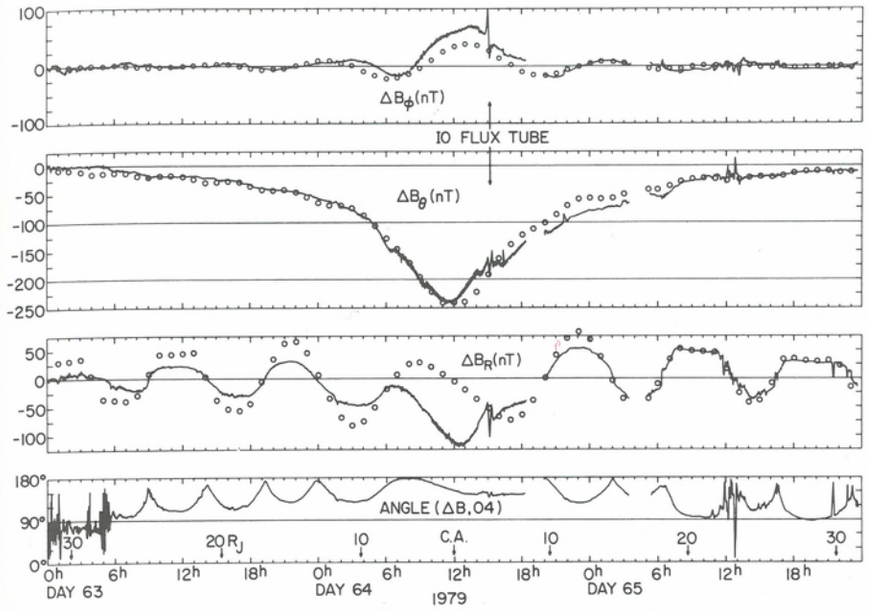

Fig. 1.21. Comparison of modeled perturbation magnetic field with that observed for Voyager 1. Open circles are (hourly) computed values using the Voyager 1 and Pioneer 10 model parameters of Connerney, Acuña, and Ness [1981].

inversely proportional to radial distance, extending from 5 to 50 R_J in the magnetic equatorial plane. Computation of the field quantities is accomplished by numerical integration, but excellent analytical approximations (for all but a small region near the inner sheet edge) can also be applied. These are given in Appendix A. A model fit to the V 1 and P 10 vector observations required a current density at the inner edge of the annulus of $\sim 5 \times 10^6\ \mathrm{A}/R_J^2$ ($\sim 1\ \mathrm{mA/km^2}$). The same model fit to the V 2 observations required $\sim 1/3$ less current. A comparison of the model fit to the V 1 perturbation field illustrated earlier appears in Figure 1.21. These simple azimuthally symmetric models are capable in each case of producing a generally good and self-consistent fit to all three field components. Details of the perturbation plots, such as the flattening of the B_r component that occurs when the spacecraft exits the current-carrying region (e.g., V 1 outbound at 0730 on Day 65), appear quite naturally in the modeled field as well. The magnetic field morphology of the annular current disc used in these models is illustrated in Figure 1.22. The magnetic field of the azimuthal sheet current has a vertical component that is antiparallel to the internal Jovian field. The total magnetospheric magnetic field, consisting of the internal Jovian dipole ($4.2\ \mathrm{G}R_J^3$) and the contribution due to the sheet currents, is illustrated in Figures 1.23 and 1.24. The field morphology is quite similar to that envisioned by the early P 10 investigators (e.g., Van Allen et al. [1974a]) with respect to the distention of field lines along the symmetry plane of the azimuthal current sheet.

A much improved fit to the V 1 observations (compare Figures 1.4 and 1.21) has been obtained (Connerney, Acuña, and Ness, 1982) by simultaneous inversion of both the internal field and the field due to the magnetodisc currents. The best fitting magnetodisc is similar to that described above, but lies in the centrifugal equator, 2/3 of the way between the rotational and magnetic equators.